HHS Public Access

Author manuscript

J Alzheimers Dis. Author manuscript; available in PMC 2017 August 31.

Published in final edited form as:

J Alzheimers Dis. 2016 ; 50(1): 133–148. doi:10.3233/JAD-150751.

Tobacco Smoke-Induced Brain White Matter Myelin Dysfunction: Potential Co-Factor Role of Smoking in Neurodegeneration

Rosa Yu[a,b,d], **Chetram Deochand**[a,b,d,h], **Alexander Krotow**[h], **Raiane Leão**[i], **Ming Tong**[a,b,d], **Amit R. Agarwal**[j], **Enrique Cadenas**[j], and **Suzanne M. de la Monte**[a,b,c,d,e,f,g,*]

[a]Liver Research Center, Divisions of Rhode Island Hospital and the Warren Alpert Medical School of Brown University, Providence, RI, USA

[b]Gastroenterology and Rhode Island Hospital and the Warren Alpert Medical School of Brown University, Providence, RI, USA

[c]Neuropathology, and Departments of Rhode Island Hospital and the Warren Alpert Medical School of Brown University, Providence, RI, USA

[d]Medicine, Rhode Island Hospital and the Warren Alpert Medical School of Brown University, Providence, RI, USA

[e]Pathology, Rhode Island Hospital and the Warren Alpert Medical School of Brown University, Providence, RI, USA

[f]Neurology, Rhode Island Hospital and the Warren Alpert Medical School of Brown University, Providence, RI, USA

[g]Neurosurgery, Rhode Island Hospital and the Warren Alpert Medical School of Brown University, Providence, RI, USA

[h]Molecular Pharmacology and Physiology Graduate Program at Brown University, Providence, RI, USA

[i]Federal University of Minas Gerais, Belo Horizonte, Minas Gerais, Brazil

[j]Department of Pharmacology and Pharmaceutical Sciences, School of Pharmacy, University of Southern California, Los Angeles, CA, USA

Abstract

Background—Meta-analysis studies showed that smokers have increased risk for developing Alzheimer's disease (AD) compared with non-smokers, and neuroimaging studies revealed that smoking damages white matter structural integrity.

*Correspondence to: Dr. Suzanne M. de la Monte, MD, MPH, Pierre Galletti Research Building, Rhode Island Hospital, 55 Claverick Street, Room 419, Providence, RI 02903, USA. Tel.: +1 401 444 7364; Fax: +1 401 444 2939; Suzanne_DeLaMonte_MD@Brown.edu.

Authors' disclosures available online (http://j-alz.com/manuscript-disclosures/15-0751rl).

SUPPLEMENTARY MATERIAL

The supplementary material is available in the electronic version of this article: http://dx.doi.org/10.3233/JAD-150751.

Objective—The present study characterizes the effects of side-stream (second hand) cigarette smoke (CS) exposures on the expression of genes that regulate oligodendrocyte myelin-synthesis, maturation, and maintenance and neuroglial functions.

Methods—Adult male A/J mice were exposed to air (8 weeks; A8), CS (4 or 8 weeks; CS4, CS8), or CS8 followed by 2 weeks recovery (CS8 + R). The frontal lobes were used for histology and qRT-PCR analysis.

Results—Luxol fast blue, Hematoxylin and Eosin stained histological sections revealed CS-associated reductions in myelin staining intensity and narrowing of the corpus callosum. CS exposures broadly decreased mRNA levels of immature and mature oligodendrocyte myelin-associated, neuroglial, and oligodendrocyte-related transcription factors. These effects were more prominent in the CS8 compared with CS4 group, suggesting that molecular abnormalities linked to white matter atrophy and myelin loss worsen with duration of CS exposure. Recovery normalized or upregulated less than 25% of the suppressed genes; in most cases, inhibition of gene expression was either sustained or exacerbated.

Conclusion—CS exposures broadly inhibit expression of genes needed for myelin synthesis and maintenance. These adverse effects often were not reversed by short-term CS withdrawal. The results support the hypothesis that smoking contributes to white matter degeneration, and therefore could be a key risk factor for a number of neurodegenerative diseases, including AD.

Keywords

Alzheimer’s disease; cigarette smoke; mouse model; myelin genes; neurodegeneration; tobacco; white matter

INTRODUCTION

Alzheimer’s disease (AD) is largely sporadic in occurrence, indicating that factors other than genetics can strongly influence its onset and progression. Therefore, in order to stymie the AD epidemic, efforts should be placed on identifying modifiable or preventable pathogenic co-factors associated with environmental and lifestyle exposures. Growing evidence supports the concept that AD is largely a brain metabolic disorder with molecular and biochemical features that are shared with diabetes mellitus and other insulin resistance diseases [1–4]. Furthermore, epidemiological studies revealed that obesity, diabetes, non-alcoholic fatty liver disease, and other insulin resistance disease states significantly increase rates of cognitive impairment [5–9]. These phenomena could reflect consequences of multiorgan targeting by a single disease mechanism, similar to the effects of chronic arterial hypertension or diabetes mellitus. Although chronic high calorie and fat intake are regarded as major culprits in the obesity epidemic, the non-linear nature of the correlation suggests other factors are likely involved.

Over the past several years, we have attended to the role of low-dose nitrosamine exposures as causal or contributory pathogenic agents of insulin resistance diseases, including neurodegeneration [10–17]. This concept was inspired by the finding that intracerebral administration of streptozotocin causes neurodegeneration with cognitive impairment, brain insulin/insulin-like growth factor (IGF) resistance, neuroinflammation, and dysregulated

metabolism [18–24] as occur in AD [4,25–28], yet when delivered systemically, streptozotocin causes diabetes mellitus [29, 30] and steatohepatitis [31, 32]. These concepts were finally interconnected by the realization that streptozotocin is a nitrosamine [29] that exerts genotoxic effects [33].

Subsequent studies were constructed to determine if other nitrosamines to which humans are commonly exposed produce toxic, degenerative, and insulin resistance effects like streptozotocin. Experiments employing N-nitrosodiethylamine (NDEA) [11, 13, 14], and later, 4-(methylnitrosamino)-1-(3-pyridyl)-1-butanone(NNK) [12,15–17] demonstrated that limited sub-mutagenic exposures to other nitrosamines also cause insulin resistance disease states. The experimental animals developed type 2 diabetes, steatohepatitis, and cognitive impairment with neurodegeneration. In humans, NDEA exposures occur via agricultural use of nitrate-containing fertilizers and consumption of nitrate- and nitrite-containing processed, preserved, or cured foods, especially meats [5, 34]. NNK and its metabolites are the most abundant and toxic nitrosamines in tobacco smoke [35–38].

The next step was to extend this line of investigation using environmentally relevant complex toxins that contain the agents of interest. In this regard, we sought to determine if tobacco smoke can cause white matter (WM) degeneration with structural and molecular abnormalities similar to those occurring after NNK exposures [12,17]. In support of this concept, chronic cigarette smoking was previously linked to cognitive impairment [39–41] and brain atrophy (neuroimaging) [42–51] affecting WM [41,49, 52]. Furthermore, meta-analyses have shown that smoking is associated with atrophy of brain regions targeted by AD [53], and that individuals with AD have higher rates of cigarette smoking than controls [54]. The present study focuses on the mechanisms of cigarette smoke (CS) induced WM degeneration. The rationale for this approach is supplied by the aforementioned human studies, together with the growing evidence that WM degeneration is an early and integral component of AD [55–61] and other neurodegenerative diseases [41, 62–66]. Herein, we characterize the effects of CS exposures and short-term withdrawal on the expression of immature and mature myelin-associated genes, neuroglial genes needed for axonal maintenance, plasticity and repair, and transcription factors that regulate neuroglial functions.

MATERIALS AND METHODS

Experimental model

These studies utilized an A/J mouse model similar to the one developed in 2002 [67]. The A/J strain was used because of their high susceptibility to lung defects after tobacco smoke exposure [68]. Furthermore, the A/J model replicates the human experience in that following chronic (5 months) tobacco smoke exposure, plasma cotinine levels are comparable to those in active human smokers, and the mice develop emphysema and lung tumors [67,69]. However, the relatively short-term exposures that we employed herein do not produce these end-point diseases [69–71]. Adult (8 weeks old) A/J male mice (N= 5–6/group) were exposed to cigarette smoke (CS) or air as follows: 1) 8 weeks of room air only (A8); 2) 4 weeks CS (CS4); 3) CS8; 4) CS8 followed by 2 weeks recovery (CS8 + R) [70, 71]. CS was generated from research grade Kentucky 3R4F cigarettes (Tobacco Research Institute,

University of Kentucky, Lexington, KY) using an industry standard Teague Enterprises, TE-10 Smoking Machine (Davis, CA). The cigarettes contained 11 mg of total particulate matter (TPM) and 0.73 mg of nicotine. Side-stream and mainstream smoke were mixed in a ratio of 89% to 11%, which is similar to environmental tobacco smoke exposures. Six cigarettes were puffed simultaneously, one time per minute for 9 puffs. The cigarettes were burned for 6 hours/day, 5 days/week and for 4 or 8 weeks duration. Mice were adapted to CS by ramping up concentration and exposure period in the first week. The chamber atmosphere was monitored for total suspended particles. The smoke exposure system involved burning of cigarettes in one location, and then delivering the smoke to exposure chambers that housed the mice. In the vicinity where cigarettes were burned, the CO levels reached 24 ppm, which is well above natural air (less than 0.5 ppm) but comparable to the amounts present in tobacco smoke exhaled by humans (25–30 ppm) [72]. The atmosphere within the mouse CS exposure chambers had 21% oxygen and approximately 3 ppm of CO. Before use, the cigarettes were kept for 48 h in a standardized atmosphere humidified with 70% glycerol-30% water. Throughout the experiment, mice were housed under humane conditions and kept on a 12-h light/dark cycle with free access to food. All experiments were performed in accordance with protocols approved by the University of Southern California's Institutional Animal Care and Use Committee, and conformed to guidelines established by the National Institutes of Health.

Brain collection and processing

Freshly harvested brains were snap-frozen and stored at −80°C. After thawing, anterior frontal lobe WM was homogenized and processed for molecular assays. An adjacent slice was immersion fixed in ice cold 4% neutral buffered paraformaldehyde containing 30% sucrose for cryoprotection. The fixed brain tissues were embedded in paraffin. Histological sections (8 μm thick) were stained with Luxol fast blue, Hematoxylin and eosin (LHE) and examined by light microscopy.

Targeted glial gene arrays

Targeted quantitative reverse transcriptase polymerase chain reaction (RT-PCR) amplification arrays were used to measure 28 mRNA transcripts corresponding to genes involved in glial and neuronal growth, maturation, and function (see Supplementary Table 1 for gene functions). The objective was to evaluate CS exposure effects on genes that are relevant to central nervous system (CNS) myelin and WM rather than the entire database of genes. PCR primer pairs were designed with Primer 3 (http://www.ncbi.nm.gov/tools/primer-blast/) software (Supplementary Table 2).Targeted arrays were constructed by spotting and drying primer pairs (100 nmol/5 μl) into individual wells of a Lightcycler 480 Multi-well Plate 96 (Roche. Indianapolis. IN). The arrays were sealed and stored at −80°C. On the day of use, the array plates were thawed on ice and 20 μl of reaction cocktail containing cDNA from 5 μg RNA template and Sybr green master mix were added to each well. PCR reactions were performed in a Roche Lightcycler 480 System. Gene expression was analyzed using the $^{\Delta\Delta}C_t$ method with results normalized to control genes (Hypoxanthine-guanine phosphoribosyltransferase. HPRT; and Ribonuclear protein. RNP) as per the SA Biosciences protocol (Qiagen. Valencia. CA). In addition, we used heatmaps to visualize clustered or patterned results.

Statistics

Inter-group comparisons were made using one-way analysis of variance (ANOVA) with Tukey *post hoc* test (GraphPad Prism 6, San Diego. CA). F-ratios and *p*-values are tabulated (Table 1). Significant post-test differences ($p < 0.05$) and trends ($0.05 < p < 0.10$) are shown in the graphs. Heatmaps were constructed using Version 3.2 of R software [73, 74]. Exploratory data analysis verified the quality of observed data. The data were imported into R as a comma delimited values table, excluding the control genes (Actin and HPRT). Several transformations were applied to the row values. To scale the data, row means were subtracted from each cell. The resulting values were further divided by the standard deviation in order to obtain a z-score of each individual cell yielding row values with a mean of 0 and S.D. of 1. The resulting values were plotted using a cosmetically modified version of a latent R heatmap function using a 6-color palette. We also applied hierarchical clustering algorithm using Euclidean distance function on the overall table to display a dendrogram of mRNAs.

RESULTS

CS-induced white matter abnormalities

Formalin-fixed, paraffin-embedded LHE stained sections of brain revealed CS exposure associated reductions in myelin staining intensity and thickness of the anterior corpus callosum relative to A8 control samples (Fig. 1). Short-term recovery from the CS exposures did not result in any detectable reversal of the WM atrophy and myelin pallor. CS-associated myelin pallor could have been due to demyelination, impaired myelin maintenance, and/or loss of myelinated fibers. Further molecular studies helped clarify the status of oligodendrocyte-associated myelin gene expression and function.

Adverse effects of CS exposures on immature and mature oligodendroglial gene expression

As markers of immature oligodendroglia, we measured nestin, vimentin, 2′,3′-Cyclic Nucleotide 3′ Phosphodiesterase (CNP), platelet-derived growth factor receptor-alpha (PDGFR-α), galactocerebroside (Gal-C), and Prominin 1 (PROM1). For mature myelinating oligodendroglia, we measured mRNA levels of proteolipid protein 1 (PLP-1), myelin oligodendrocyte glycoprotein 1 (MOG-1), myelin-associated glycoprotein 1 (MAG-1), myelin basic protein (MBP), Reticulon 4 (RTN4), RPA interacting protein (RPAIN), and ST8 alpha-N-acetylneuraminidealpha-2,8-sialytransferase 1 (ST8SIA1). One-way repeated measures ANOVA tests demonstrated significant CS exposure effects on most of the immature (CNP, GAL-C, nestin, and PDGFR-α) and mature (MAG-1, MBP, PLP, RPAIN, RTN4, and ST8SIA1) oligodendroglial genes, and a trend effect ($0.05 < p < 0.10$) on MOG (Table 1).

The graphed results and post-hoc tests demonstrated significant reductions in nestin (Fig. 2A) and CNP (Fig. 2C) expression in CS8 and CS8 + R relative to A8 and CS4, and significant reductions in PDGFR-α expression in CS8 + R relative to A8, CS4, and CS8 (Fig. 2D). A statistical trend was detected for increased levels of PROM1 mRNA in CS8 + R relative to CS4 and CS8 (Fig. 2F). Gal-C elevation in CS4 caused the difference from CS8 to

be statistically significant (Fig. 2E). In contrast, vimentin expression was not significantly modulated by CS exposure (Fig. 2B). Overall, the main inhibitory effects on immature oligodendroglial genes occurred in the CS8 and CS8 + R groups.

Among the mature oligodendroglial genes, only PLP-1 was upregulated in CS8 + R relative to A8, CS4, and CS8, which had similar mRNA levels (Fig. 3A). With respect to RTN4, CS8 + R had precisely the opposite effect, manifested by selective inhibition of gene expression relative to A8, CS4, and CS8 (Fig. 3E). MAG-1 (Fig. 3C) and ST8S1a-1 (Fig. 3G) mRNA levels were unaffected by CS4, but significantly and similarly reduced by CS8 and CS8 + R. The expression levels of both MOG-1 (Fig. 3B) and RPAIN (Fig. 3F) declined progressively from A8 to CS4, then CS8, and finally CS8 + R. MBP was the only gene whose expression was significantly reduced in all CS groups relative to control (Fig. 3D).

CS exposures alter neural-glial gene expression

The analyses were extended to examine effects of CS exposures and withdrawal on selected neuronal and astrocytic genes. To do this, we measured mRNA levels of Chondroitin Sulfate Proteoglycan 4 (CSPG4), GEAP, Glycerol-3-phosphate dehydrogenases 1 and 2 (GPD1, GPD2), Glutathione S-Transferase Pi-1 (GSTP1), neural cell adhesion molecule (NCAM), and neurotrophic tyrosine kinase receptor, Type 2 (NTRK2). One-way ANOVA tests demonstrated significant CS exposures effects on GFAP, GSTP1, NCAM, and NTRK2, trend effects on CSPG4 and GPD1, and no effect on GPD2 (Table 1). The combined modest stimulatory effect of CS4 and inhibitory effect of CS8 + R on CSPG4 rendered those differences statistically significant (Fig. 4A). GEAP was the only other mRNA that was upregulated by CS4, resulting in higher levels of expression relative to A8, CS8, and CS8 + R (Fig. 4B). The expression levels of NCAM (Fig. 4 C), GPD1 (Fig. 4E), and GSTP1 (Fig. 4 G) gradually declined from A8 to CS4, then CS8, such that the differences between A8 and CS8 were statistically significant. CS8 + R exposures had widely disparate effects, normalizing NCAM, not affecting GPD1, and further inhibiting GSTP1. CS8-mediated inhibition of GPD2 expression was abrogated by CS withdrawal, normalizing the mRNA levels and resulting in significantly higher expression in CS8 + R relative to CS8 (Fig. 4F). Finally, NRTK2 expression was similar in the A8, CS4 and CS8 groups, and selectively reduced by CS8 + R(Fig.4D).

CS exposures alter glial transcription factor gene expression

We measured frontal lobe mRNA levels of Fork-head Box 01 (FOXO1), FOXO4, oligodendrocyte transcription factor 1 (Olig1), Olig2, NK2 Homeoboxes 2 and 6 (NKX2-2, NKX6), Paired box 6 (PAX6), and Sex determining region Y-Box 9 (SOX9). One-way ANOVA tests demonstrated significant CS effects on all but FOXO1. NKX2-2, and SOX9 (Table 1). Post-hoc Tukey tests revealed that CS8 and CS8 + R significantly reduced expression of FOXO4 (Fig. 5B), Olig1 (Fig. 5C), Olig2 (Fig. 5D), and NKX6-1 (Fig. 5F) relative to A8 or CS4. Although the CS4-associated increases in Olig2, NKX2-2, and NKX6-1 expression were modest and not statistically significant relative to control, the differences between CS8/CS8 + R and CS4 were more pronounced than the differences relative to A8. This phenomenon was particularly evident in regard to NKX2-2 (Fig. 5E). PAX6 expression gradually declined from A8 to CS4 to CS8, but short-term CS withdrawal

completely reversed this trend, increasing the expression levels above control (Fig. 5G). There were no significant CS effects on FOXO1 (Fig. 5A) or SOX9 (Fig. 5 H) expression.

Heatmaps depict differential CS dose/duration and withdrawal effects on gene expression levels

Heatmaps with hierarchical clustering helped to illustrate overall effects of CS exposures on frontal lobe expression of immature and mature oligodendroglial, neuroglial, and transcription factor genes (Fig. 6). The overall heatmap that included all genes evaluated identified three main hierarchical clusters (CNP to GSTP1; NKX6 to MAG-1; and MBP to NRTK2) that all had similar trends. In those clusters, the highest levels of gene expression occurred in the A8 or CS4 groups, and consistently lower levels marked CS8 or CS8 + R exposures. Furthermore, gene expression was generally higher in A8 than CS4. and in CS8 than CS8 + R. This suggests that the inhibitory effects of CS increase with longer durations of CS exposure and/or the interval from initialing CS exposures. The uppermost cluster (IV; from PROM to NCAM) was associated with intermediate levels of gene expression in A8 controls, reduced expression in the CS4 and/or CS8 groups, and either normalized or above-normal levels of gene expression in the CS8 + R group. The fifth and lowermost cluster (from CSPG4 to SOX9) showed CS4-associated increases in gene expression, variable effects of CS8 including normalization, suppression, or further enhancement of gene expression, and mainly suppressed gene expression in the CS8 + R group.

We generated data subset heatmaps to better appreciate the effects of CS on immature (Supplementary Fig. 1A) and mature oligodendroglial (Supplementary Fig. 1B) genes, neuroglial markers (Supplementary Fig. 1C). and transcription factors (Supplementary Fig. 1D). Among the immature oligodendroglial genes (Supplementary Fig. 1A). roughly three clustered effects of CS and CS+R were evident. The uppermost row (PROM) and the lowest two rows (GAL-C and Vimentin) had nearly reciprocal trends in that for PROM, gene expression was intermediate for controls, sharply reduced by CS4 and CS8. and highest in the CS8 + R, reflecting a reversal and overcorrection of CS suppression. In contrast, for GAL-C and Vimentin. gene expression was relatively low in controls, upregulated by CS4. either inhibited (GAL-C) or further stimulated (Vimentin). and downregulaled (normalized or over-corrected) by CS8 + R. The middle cluster corresponding to Nestin, CNP, and PDGFR-α was clearest in that A8 and CS4 had high levels of gene expression, while CS8 and CS8 + R exposures sharply reduced gene expression. Therefore, except for PROM and Vimentin. CS8 and CS8 + R exposures broadly reduced expression of immature oligodendroglial gene, whereas CS4 exposure responses were more varied.

The dominant clustered effect of all CS exposures on mature oligodendroglial genes was suppression of MBP, RPA1N, and MOG whereby gene expression was reduced to similar or greater degrees in CS8 compared with CS4, and in CS8 + R compared with CS8 (Supplementary Fig. 1B). The second cluster was associated with CS8 and CS8 + R mediated suppression of ST8 and MAG relative to A8 and CS4. Apart from the CS4-associated stimulation, RTN4 also clustered with MBP, RPAIN, and MOG, and profiles. The effects of CS exposures and recovery were reciprocal for PLP and RTN4. For PLP, CS4 inhibited while CS8 + R sharply stimulated gene expression relative to control, whereas for

RTN4, CS4 stimulated while CS8 + R decisively inhibited gene expression. In essence, the overall trends with respect to mature oligodendroglial genes were that CS exposures reduced gene expression, and that longer durations of CS exposure (CS8) or interval from initiating the CS exposures (CS8 + R) had greater inhibitory effects than CS4 (Supplementary Fig. 1B). PLP was the exception in that CS8 + R exposures strikingly upregulated its expression.

The neuroglial heatmap had revealed complex trends and clustering of gene responses to CS exposures (Supplementary Fig. 1 C). The CSPG4/GFAP cluster was characterized by pronounced CS4 stimulation. and CS8 and CS8 + R inhibition of gene expression relative to control. The GSTP1/GPD1 cluster was associated with progressive reductions in gene expression from A8 to CS4 and then CS8. with no further reductions associated with CS8 + R. CS effects on NRTK2 were distinct from the other clusters. Finally. GPD2 and NCAM were clustered by the marked CS8-mediated reductions in gene expression, together with CS8 + R-mediated upregulation with normalization or over-correction of gene expression relative to control. Therefore, for the most part, CS exposures (especially CS8 and CS8 + R) inhibited neuroglial gene expression, and in just 2 of the 7 genes, the suppressive effects were abrogated by short-term CS withdrawal.

The transcription factor heatmap had three main hierarchical clusters (Supplementary Fig. 1D). The uppermost cluster, including FOXO1 and PAX6, exhibited roughly reciprocal CS responses compared with the lowermost cluster, including NKX2 and SOX9. CS4 and CS8 mainly suppressed FOXO1 and PAX6 which CS8 + R sharply upregulated these genes relative to control. In contrast, CS4 and CS8 mainly stimulated NKX2 and SOX9, which CS8 + R sharply reduced their expressions. The middle hierarchical cluster showed higher levels of NKX6, OLIG1, OLIG2, and FOXO4 in A8 and CS4 brains with some stimulatory effects of CS4 (NKX6 and OLIG2), and consistently lower levels of gene expression in the CS8 and CS8 + R groups. Therefore, as was the case for immature and mature oligodendroglial and neuroglial genes, with limited exceptions, CS exposures broadly inhibited expression of transcription factor genes, and a brief period of CS withdrawal mainly either further reduced or failed to abrogate the inhibitory effects of CS8.

DISCUSSION

Nitrosamines and tobacco toxins as mediators of insulin/IGF-1 resistance diseases

Tobacco smoke contains hundreds of toxins, including volatile, non-volatile, and tobacco-specific nitrosamines. Although the main focus of our research is to study the role of tobacco-specific nitrosamine-mediated WM degeneration, comparing direct (NNK) with indirect (CS) effects, carbon monoxide (CO) also has the potential to cause WM injury [75]. Fortunately, the experimental design was such that the maximum CO level reached within the chambers that housed the mice was approximately 3 ppm, which is comparable to human cigarette smoking exposures. CO levels in natural air are less than 0.5 ppm, whereas the amount exhaled by regular tobacco smokers is on the order of 25 or 30 ppm [72]. Environmentally tolerable CO levels can be as high as 70 ppm. CNS toxicity occurs at 150 or 200 ppm of CO [76]. CO neurotoxicity is manifested by delirium, loss of consciousness, or death due to hypoxic-ischemic encephalopathy leading to progressive WM degeneration

and death of iron-rich neurons in the globus pallidus and substantia nigra [75]. Under the experimental conditions employed herein, the risk of CO neurotoxicity was nil.

The most potent and abundant tobacco-specific nitrosamines in CS are NNK and NNN [38, 77, 78]. A single cigarette has between 1 μg and 9 μg of tobacco-specific nitrosamines and up to 8 μg of other classes of nitrosamines, and it releases up to 2 μg of nitrosamine products into the air [79]. Therefore, nitrosamine exposures via first- and second-hand smoke are significant. However, the study design did not include measurement of tobacco nitrosamine levels in the chamber. Although the vast majority of research on nitrosamine-induced diseases is focused on carcinogenesis, our research has led to the concept that low-level nitrosamine exposures also threaten health by causing progressive degenerative diseases linked to impairments in insulin/IGF signaling through cell survival and metabolic pathways, dysregulated lipid metabolism, tissue injury, inflammation, and oxidative and nitrosative stress [11, 14, 80]. In this regard, we have already shown that low-level NNK or NDEA exposures cause steatohepatitis and neurodegeneration, and that those effects can be exacerbated by co-exposures to alcohol or high fat diets, which themselves cause insulin/IGF resistance, cellular stress, and inflammation [12, 14, 16]. Our recent studies demonstrated significant WM degeneration with inhibition of insulin and IGF-1 signaling and expression of oligodendroglial/myelin-associated genes, and striking alterations in phospholipid and sphingolipid profiles in brains of NNK-exposed rats [12, 15, 17]. Regarding the present study, many WM abnormalities produced by NNK also occurred following CS exposure, supporting the hypothesis that nitrosamines, including those present in CS, can mediate WM degeneration.

The present study circles back to the main clinical and epidemiological concerns regarding effects of CS exposures on the brain. We directed our attention to WM because: 1) WM atrophy is an early and consistent feature of AD as well as other neurodegenerative diseases; 2) WM atrophy is linked to cognitive impairment; 3) oligodendrocyte survival and function are regulated by insulin and IGF signaling; 4) smoking is a risk factor for AD; 5) AD is associated with many abnormalities in myelin-associated lipids and gene expression; and 6) experimental exposures to various nitrosamines, including NNK, impair oligodendroglial gene expression and function.

CS-associated white matter pathology

Histopathological studies demonstrated that CS exposures caused WM atrophy and pallor of myelin staining. The latter reflects loss of myelin due to demyelination or impaired myelin maintenance and maturation. These effects of CS are reminiscent of AD-associated WM pathology which ranges from pallor of myelin staining to leukoaraiosis with attrition of myelinated axons, as was first reported by Brun and England [55, 56, 81, 82], and later shown to be present at early, pre-clinical stages of AD [57]. In AD, WM degeneration is associated with partial loss of myelin sheaths, axons, and oligodendroglial cells [55], which could be mediated by myelin breakdown due to increased susceptibility of oligodendrocytes to free radical and other metabolic damage [83]. Alternatively, WM degeneration could be caused by impaired survival of oligodendrocytes with attendant expansion of astrocyte populations [84], decreased myelin density [85], and downregulated expression of MBP

[86]. We addressed mechanisms of CS-induced WM atrophy and myelin pallor using a targeted array to measure mRNA transcripts corresponding to immature and mature oligodendroglial functions, including myelin-associated gene expression.

Oligodendroglial genes-lineage, maturation, and function

Oligodendroglial cells produce CNS myelin, whose main function is to ensure efficient conductivity in nerve cells. Oligodendrocytes develop from precursor cells (OPC 1–3) that differentially express 2′,3′-cyclic nucleotide 3′ phosphodiesterase (CNP), NG2 proteoglycan (chondroitin sulfate proteoglycan 4; CSPG4), Platelet Derived Growth Factor Receptor, alpha polypeptide (PDGFR-α), Oligodendrocyte Transcription Factor 2 (Olig2), Dlx2 Homeobox, and NK2 Homeobox (Nkx) (Supplementary Table 1). OPCs differentiate into immature oligodendroglia expressing CNP, Olig1, and low levels of Olig2, followed by CNP, Olig1, low Olig2, and Reticulon 4 (RTN4) [87–89]. Myelinating mature oligodendroglia express characteristic integral membrane proteins including, myelin basic protein (MBP), myelin associated glycoprotein (MAG-1), myelin oligodendrocyte glycoprotein (MOG), and proteolipid protein (PLP) [90, 91].

Oligodendrocyte genes needed for myelin maintenance, maturation, and function are impaired by CS exposures

Targeted arrays were mainly focused on oligodendroglial-associated genes. The results were interpreted by clustering data according to: 1) genes expressed in immature versus mature oligodendrocytes; 2) other neuroglial genes; and 3) transcription factors. The combined utilization of ANOVA tests and heatmaps facilitated identification of major trends. CS4 exposures had no significant effect on the expression of immature oligodendroglial genes, whereas 8 weeks of CS exposure were inhibitory for Nestin and CNP relative to A8 and CS4. Short-term CS withdrawal failed to abrogate inhibitory effects of CS8 on immature oligodendroglial gene expression, and further reduced of PDGFR-α expression.

Nestin regulates vimentin intermediate filament disassembly during growth and is needed for survival, renewal, and proliferation of neural progenitor cells. Inhibition of Nestin could reflect CS-mediated impairments in neurogenesis. CNP is a myelin associated marker of oligodendrocytes that may play an important role in the development of myelin membranes and maintenance of axonal integrity. The inhibitory effects of CS8 and CS8 + R on CNP suggest that prolonged CS exposures impair myelin synthesis. Therefore, CS-associated WM atrophy could have been caused by reduced myelin maintenance. PDGFR-α is a cell surface receptor tyrosine kinase expressed in oligoprogenitor cells. PDGF stimulation of PDGFR-α activates proliferation pathways. Altogether, the results suggest that the CS8 exposures inhibit expression of genes needed for proliferation of immature oligodendroglia and the generation of myelin. The sustained or further impairments in gene expression observed in the CS8 + R group indicate that the adverse effects of CS8 were not reversed by short-term CS withdrawal. Moreover, CS-mediated impairments in oligodendroglial gene expression and attendant WM atrophy and degeneration may progress over time once the cascade is established. This would suggest that besides smoking cessation, other interventions may be needed to halt WM degeneration.

In general, CS exposures broadly inhibited the expression of mature oligodendroglial genes. The patterns could be summarized as follows: 1) gene expression declined from CS4 to CS8, with (MOG-1 and RPAIN) or without (MAG-1 and ST8Sla-1) further reductions in the CS8 + R group; 2) gene expression was similar among the A8, CS4, and CS8 groups, but sharply higher (PLP-1) or lower (RTN4) in the CS8 + R group; and 3) gene expression was inhibited by CS, irrespective of duration or withdrawal (MBP). In essence, PLP-1 was the single exception whereby CS exposures upregulated gene expression, and that response occurred in the CS8 + R group. In aggregate, CS exposures mainly and overwhelmingly inhibited expression of both immature and mature oligodendrocyte myelin-associated genes that are needed to generate and maintain mature myelin. Failure of processes needed for maturation and maintenance of CNS myelin could compromise axonal functions and contribute to neurobehavioral deficits that occur with smoking. On the other hand, given the role of PLP-1 in compaction, stabilization, and maintenance of myelin sheaths, the findings suggest that CS recovery can enhance the structural integrity of myelin.

Complex effects of CS exposures on neuroglial genes

The only significant effect CS4 had on neuroglial gene expression was to increase GFAP. In contrast, CS8 and/or CS8 + R significantly reduced expression of NCAM, GPD1, GSTP1, and NRTK2 relative to A8. CS withdrawal abolished the inhibitory effects of CS8 on NCAM and GPD2. These CS effect trends were better appreciated from the graphs together with the heatmap which demonstrated CS4-stimulation and CS8 and CS8 + R inhibition of CSPG4 and GFAP relative to control, and progressive declines in NCAM, GPD1, GPD2, and GSTP1 expression from A8 to CS4 and then CS8. CS8 + R responses varied in that the levels of gene expression relative to CS8 were sustained (GFAP, GSTP1, GPD1), further inhibited (CSPG4, GSTP1), or abrogated (NCAM, GPD2). Since CSPG4 inhibits neurite outgrowth and promotes growth cone collapse during axon regeneration [92, 93], the higher expression with CS4 and normalization or inhibition with CS8 and CS8 + R suggest the initial responses to CS exposures are toxic and damaging to neuronal plasticity, whereas longer CS exposures may lead to adaptive downregulation of the gene. In contrast, CS4 and CS8 inhibited NCAM1 which mediates neuronal adhesion and neurite outgrowth [94, 95], while CS8 + R inhibited NTRK2, a positive regulator of synapse formation and plasticity [95]. The inhibitory effects of CS on GSTP1 (glutathione-S-transferase pi 1), which negatively regulates p25 activation of CDK5, preventing neurodegeneration, provide further evidence that CS exposures impair neuronal plasticity. The CS-associated declines in GPD1 may reflect decreased oligodendroglial tolerance to oxidative stress, rendering the cells more vulnerable to injury and death. Altogether, the findings with respect to neuroglial genes suggest that CS exposures promote neurodegeneration by impairing processes needed for neuronal plasticity, repair, and adaptive responses to stress.

CS effects on transcription factor genes—potential relevance to associated insulin signaling abnormalities

The effects of CS exposure on transcription factors were complex such that the overall trends were best revealed by the heatmap. Olig1 and Olig2, which promote formation and maturation of oligodendrocytes, were inhibited in the CS8 and CS8 + R groups relative to control and/or CS4. This effect could result in CS-associated declines in the oligodendrocyte

population and mature myelin maintenance, as suggested by the correspondingly reduced expression levels of mature myelin-associated genes. FOXO4 and NKX6 mRNA levels were higher in the A8 and CS4 compared with CS8/CS8 + R, whereas FOXO1 expression decreased sharply with CS4 exposures, but increased with CS8 followed by CS8 + R exposures and NKX2 exhibited no discernible pattern. FOXO1 and FOXO4 target insulin signaling [96]. NKX2-2 and NKX6-1 cooperate in regulating regions of axon guidance and support insulin-producing cells [97], myelin maturation from OPCs [98], and genes that have important roles in axonal guidance [99]. Therefore, at least with respect to FOXO4 and NKX6, CS8/CS8 + R could adversely affect the regulation of insulin-mediated functions in the brain. The findings suggest that the longer duration CS exposures, independent of short-term withdrawal, can contribute to WM degeneration by impairing oligodendrocyte survival and function, which are positively regulated by insulin/IGF signaling. However, the finding that CS withdrawal reversed CS-inhibition of FOXO1 and PAX6 expression suggests that even short-term smoking cessation could help restore insulin signaling, myelinogenesis, and myelin maintenance.

The strengths of this research are that the investigations are novel and they explore the molecular pathogenesis of WM degeneration associated with CS exposure. Furthermore, in light of CS's adverse effects on the expression of oligodendrocyte and myelin-associated genes, this study illustrates how CS exposures could contribute to WM degeneration in AD. The weaknesses are that the CS exposures were relatively short and therefore did not permit correlation with the emergence and progression of emphysema/chronic obstructive pulmonary disease and associated hypoxia. In addition, the study was limited to WM. Future studies should be extended to gray matter structures that are degenerated in AD.

Supplementary Material

Refer to Web version on PubMed Central for supplementary material.

Acknowledgments

Supported by AA-11431, AA-12908 and a Diversity Supplement to AA-11431 from the National Institutes of Health, and the Tobacco-Related Disease Research Program Grant 17RT-0171.

References

1. de la Monte SM. Brain insulin resistance and deficiency as therapeutic targets in Alzheimer's disease. Curr Alzheimer Res. 2012; 9:35–66. [PubMed: 22329651]
2. de la Monte SM. Contributions of brain insulin resistance and deficiency in amyloid-related neurodegeneration in Alzheimer's disease. Drugs. 2012; 72:49–66. [PubMed: 22191795]
3. de la Monte SM, Longato L, Tong M, Wands JR. Insulin resistance and neurodegeneration: Roles of obesity, type 2 diabetes mellitus and non-alcoholic steatohepatitis. Curr Opin Investig Drugs. 2009; 10:1049–1060.
4. Talbot K, Wang HY, Kazi H, Han LY, Bakshi KP, Stucky A, Fuino RL, Kawaguchi KR, Samoyedny AJ, Wilson RS, Arvanitakis Z, Schneider JA, Wolf BA, Bennett DA, Trojanowski JQ, Arnold SE. Demonstrated brain insulin resistance in Alzheimer's disease patients is associated with IGF-1 resistance, IRS-1 dysregulation, and cognitive decline. J Clin Invest. 2012; 122:1316–1338. [PubMed: 22476197]

5. de la Monte SM, Neusner A, Chu J, Lawton M. Epidemilogical trends strongly suggest exposures as etiologic agents in the pathogenesis of sporadic Alzheimer's disease, diabetes mellitus, and non-alcoholic steatohepatitis. J Alzheimers Dis. 2009; 17:519–529. [PubMed: 19363256]
6. Farrell GC. The liver and the waistline: Fifty years of growth. J Gastroenterol Hepatol. 2009; 24(Suppl 3):S105–S118. [PubMed: 19799688]
7. Charlton M. Nonalcoholic fatty liver disease: A review of current understanding and future impact. Clin Gastroenterol Hepatol. 2004; 2:1048–1058. [PubMed: 15625647]
8. Mensah GA, Mokdad AH, Ford E, Narayan KM, Giles WH, Vinicor F, Deedwania PC. Obesity, metabolic syndrome, and type 2 diabetes: Emerging epidemics and their cardiovascular implications. Cardiol Clin. 2004; 22:485–504. [PubMed: 15501618]
9. Pacifico L, Nobili V, Anania C, Verdecchia P, Chiesa C. Pediatric nonalcoholic fatty liver disease, metabolic syndrome and cardiovascular risk. World J Gastroenterol. 2011; 17:3082–3091. [PubMed: 21912450]
10. Andreani T, Tong M, de la Monte SM. Hotdogs and beer: Dietary nitrosamine exposure exacerbates neurodevelopmental effects of ethanol in fetal alcohol spectrum disorder. JDAR. 2014; 3:1–9.
11. de la Monte SM, Tong M. Mechanisms of nitrosamine-mediated neurodegeneration: Potential relevance to sporadic Alzheimer's disease. J Alzheimers Dis. 2009; 17:817–825. [PubMed: 19542621]
12. Tong M, Yu R, Deochand C, de la Monte SM. Differential contributions of alcohol and the nicotine-derived nitrosamine ketone (NNK) to insulin and insulin-like growth factor resistance in the adolescent rat brain. Alcohol Alcohol. 2015; 50:670–679. [PubMed: 26373814]
13. Tong M, Longato L, de la Monte SM. Early limited nitrosamine exposures exacerbate high fat diet-mediated type2 diabetes and neurodegeneration. BMC Endocr Disord. 2010; 10:4. [PubMed: 20302640]
14. Tong M, Neusner A, Longato L, Lawton M, Wands JR, de la Monte SM. Nitrosamine exposure causes insulin resistance diseases: Relevance to type 2 diabetes mellitus, non-alcoholic steatohepatitis, and Alzheimer's disease. J Alzheimers Dis. 2009; 17:827–844. [PubMed: 20387270]
15. Yalcin EB, Nunez K, Tong M, de la Monte SM. Differential sphingolipid and phospholipid profiles in alcohol and nicotine-derived nitrosamine ketone-associated white matter degeneration. Alc Clin Exp Res. 2015 in press.
16. Zabala V, Tong M, Yu R, Ramirez T, Yalcin EB, Balbo S, Silbermann E, Deochand C, Nunez K, Hecht S, de la Monte SM. Potential contributions of the tobacco nicotine-derived nitrosamine ketone (NNK) in the pathogenesis of steatohepatitis in a chronic plus binge rat model of alcoholic liver disease. Alcohol Alcohol. 2015; 50:118–131. [PubMed: 25618784]
17. Tong M, Yu R, Silbermann E, Zabala V, Deochand C, de la Monte SM. Differential Contributions of Alcohol and Nicotine-Derived Nitrosamine Ketone (NNK) to White Matter Pathology in Adolescent Rat Brains. Alcohol Alcohol. 2015; 50:680–689. [PubMed: 26373813]
18. Hoyer S. Neurodegeneration, Alzheimer's disease, and beta-amyloid toxicity. Life Sci. 1994; 55:1977–1983. [PubMed: 7997056]
19. Blum-Degen D, Frolich L, Hoyer S, Riederer P. Altered regulation of brain glucose metabolism as a cause of neurodegenerative disorders? J Neural Transm Suppl. 1995; 46:139–147. [PubMed: 8821049]
20. Hoyer S. Oxidative metabolism deficiencies in brains of patients with Alzheimer's disease. Acta Neurol Scand Suppl. 1996; 165:18–24. [PubMed: 8740985]
21. Blass JP, Gibson GE, Hoyer S. The role of the metabolic lesion in Alzheimer's disease. J Alzheimers Dis. 2002; 4:225–232. [PubMed: 12226541]
22. Gasparini L, Netzer WJ, Greengard P, Xu H. Does insulin dysfunction play a role in Alzheimer's disease? Trends Pharmacol Sci. 2002; 23:288–293. [PubMed: 12084635]
23. de la Monte SM, Tong M, Lester-Coll N, Plater M Jr, Wands JR. Therapeutic rescue of neurodegeneration in experimental type 3 diabetes: Relevance to Alzheimer's disease. J Alzheimers Dis. 2006; 10:89–109. [PubMed: 16988486]

24. Lester-Coll N, Rivera EJ, Soscia SJ, Doiron K, Wands JR, de la Monte SM. Intracerebral streptozotocin model of type 3 diabetes: Relevance to sporadic Alzheimer's disease. J Alzheimers Dis. 2006; 9:13–33. [PubMed: 16627931]
25. Rivera EJ, Goldin A, Fulmer N, Tavares R, Wands JR, de la Monte SM. Insulin and insulin-like growth factor expression and function deteriorate with progression of Alzheimer's disease: Link to brain reductions in acetylcholine. J Alzheimers Dis. 2005; 8:247–268. [PubMed: 16340083]
26. Steen E, Terry BM, Rivera EJ, Cannon JL, Neely TR, Tavares R, Xu XJ, Wands JR, de la Monte SM. Impaired insulin and insulin-like growth factor expression and signaling mechanisms in Alzheimer's disease—is this type 3 diabetes? J Alzheimers Dis. 2005; 7:63–80. [PubMed: 15750215]
27. Craft S. Insulin resistance and Alzheimer's disease pathogenesis: Potential mechanisms and implications for treatment. Curr Alzheimer Res. 2007; 4:147–152. [PubMed: 17430239]
28. de la Monte SM, Re E, Longato L, Tong M. Dysfunctional pro-ceramide, ER stress, and insulin/IGF signaling networks with progression of Alzheimer's disease. J Alzheimers Dis. 2012; 30(Suppl 2):S217–S229. [PubMed: 22297646]
29. Bolzan AD, Bianchi MS. Genotoxicity of streptozotocin. Mutat Res. 2002; 512:121–134. [PubMed: 12464347]
30. Koulmanda M, Qipo A, Chebrolu S, O'Neil J, Auchincloss H, Smith RN. The effect of low versus high dose of streptozotocin in cynomolgus monkeys (Macaca fascilularis). Am J Transplant. 2003; 3:267–272. [PubMed: 12614280]
31. Yan AG, Ge ZY, Liu JX, Dong XX, Li HK, Jin L. [Effect of Jiangtang Xiaozhi capsule on morphological changes of islet and liver in rat model [corrected] of type 2 diabetes [corrected] mellitus]. Zhongguo Thong Yao Za Zhi. 2008; 33:1067–1071.
32. Wang S, Kamat A, Pergola P, Swamy A, Tio F, Cusi K. Metabolic factors in the development of hepatic steatosis and altered mitochondrial gene expression *in vivo*. Metabolism. 2011; 60:1090–1099. [PubMed: 21310443]
33. Kaina B, Fritz G, Coquerelle T. Contribution of O6-alkylguanine and N-alkylpurines to the formation of sister chromatid exchanges, chromosomal aberrations, and gene mutations: New insights gained from studies of genetically engineered mammalian cell lines. Environ Mol Mutagen. 1993; 21:283–292.
34. Bryan NS, Alexander DD, Coughlin JR, Milkowski AL, Boffetta P. Ingested nitrate and nitrite and stomach cancer risk: An updated review. Food Chem Toxicol. 2012; 50:3646–3665. [PubMed: 22889895]
35. Trushin N, Hecht SS. Stereoselective metabolism of nicotine and tobacco-specific N-nitrosamines to 4-hydroxy-4-(3-pyridyl)butanoic acid in rats. Chem Res Toxicol. 1999; 12:164–171. [PubMed: 10027794]
36. Hoffmann D, Hecht SS, Ornaf RM, Wynder EL. N′-nitrosonornicotine in tobacco. Science. 1974; 186:265–267. [PubMed: 4414773]
37. Hecht SS, Ornaf RM, Hoffmann D. Chemical studies on tobacco smoke. XXXIII. N′-nitrosonornicotine in tobacco: Analysis of possible contributing factors and biologic implications. J Natl Cancer Inst. 1975; 54:1237–1244. [PubMed: 236398]
38. Stepanov I, Feuer R, Jensen J, Hatsukami D, Hecht SS. Mass spectrometric quantitation of nicotine, cotinine, and 4-(methylnitrosamino)-1-(3-pyridyl)-1-butanol in human toenails. Cancer Epidemiol Biomarkers Prev. 2006; 15:2378–2383. [PubMed: 17164359]
39. Durazzo TC, Gazdzinski S, Banys P, Meyerhoff DJ. Cigarette smoking exacerbates chronic alcohol-induced brain damage: A preliminary metabolite imaging study. Alcohol Clin Exp Res. 2004; 28:1849–1860. [PubMed: 15608601]
40. Durazzo TC, Gazdzinski S, Meyerhoff DJ. The neurobiological and neurocognitive consequences of chronic cigarette smoking in alcohol use disorders. Alcohol Alcohol. 2007; 42:174–185. [PubMed: 17526627]
41. Durazzo TC, Rothlind JC, Cardenas VA, Studholme C, Weiner MW, Meyerhoff DJ. Chronic cigarette smoking and heavy drinking in human immunodeficiency virus: Consequences for neurocognition and brain morphology. Alcohol. 2007; 41:489–501. [PubMed: 17923369]

42. Almeida OP, Garrido GJ, Lautenschlager NT, Hulse GK, Jamrozik K, Flicker L. Smoking is associated with reduced cortical regional gray matter density in brain regions associated with incipient Alzheimer disease. Am J Geriatr Psychiatry. 2008; 16:92–98. [PubMed: 18165464]
43. Brody AL, Mandelkern MA, Jarvik ME, Lee GS, Smith EC, Huang JC, Bota RG, Bartzokis G, London ED. Differences between smokers and nonsmokers in regional gray matter volumes and densities. Biol Psychiatry. 2004; 55:77–84. [PubMed: 14706428]
44. Das D, Cherbuin N, Anstey KJ, Sachdev PS, Easteal S. Lifetime cigarette smoking is associated with striatal volume measures. Addict Biol. 2012; 17:817–825. [PubMed: 21392170]
45. Fritz HC, Wittfeld K, Schmidt CO, Domin M, Grabe HJ, Hegenscheid K, Hosten N, Lotze M. Current smoking and reduced gray matter volume-a voxel-based morphometry study. Neuropsychopharmacology. 2014; 39:2594–2600. [PubMed: 24832823]
46. Gallinat J, Meisenzahl E, Jacobsen LK, Kalus P, Bierbrauer J, Kienast T, Witthaus H, Leopold K, Seifert F, Schubert F, Staedtgen M. Smoking and structural brain deficits: A volumetric MR investigation. Eur J Neurosci. 2006; 24:1744–1750. [PubMed: 17004938]
47. Liao Y, Tang J, Liu T, Chen X, Hao W. Differences between smokers and non-smokers in regional gray matter volumes: A voxel-based morphometry study. Addict Biol. 2012; 17:977–980. [PubMed: 20731627]
48. Paul RH, Grieve SM, Niaura R, David SP, Laidlaw DH, Cohen R, Sweet L, Taylor G, Clark RC, Pogun S, Gordon E. Chronic cigarette smoking and the microstructural integrity of white matter in healthy adults: A diffusion tensor imaging study. Nicotine Tob Res. 2008; 10:137–147. [PubMed: 18188754]
49. Gazdzinski S, Durazzo TC, Studholme C, Song E, Banys P, Meyerhoff DJ. Quantitative brain MRI in alcohol dependence: Preliminary evidence for effects of concurrent chronic cigarette smoking on regional brain volumes. Alcohol Clin Exp Res. 2005; 29:1484–1495. [PubMed: 16131857]
50. Durazzo TC, Mattsson N, Weiner MW. Alzheimer's Disease Neuroimaging I. Smoking and increased Alzheimer's disease risk: A review of potential mechanisms. Alzheimers Dement. 2014; 10:S122–S145. [PubMed: 24924665]
51. Durazzo TC, Meyerhoff DJ, Nixon SJ. A comprehensive assessment of neurocognition in middle-aged chronic cigarette smokers. Drug Alcohol Depend. 2012; 122:105–111. [PubMed: 21992872]
52. Wang JJ, Durazzo TC, Gazdzinski S, Yeh PH, Mon A, Meyerhoff DJ. MRSI and DTI: A multimodal approach for improved detection of white matter abnormalities in alcohol and nicotine dependence. NMR Biome. 2009; 22:516–522.
53. Pan P, Shi H, Zhong J, Xiao P, Shen Y, Wu L, Song Y, He G. Chronic smoking and brain gray matter changes: Evidence from meta-analysis of voxel-based morphometry studies. Neurol Sci. 2013; 34:813–817. [PubMed: 23207549]
54. Cataldo JK, Prochaska JJ, Glantz SA. Cigarette smoking is a risk factor for Alzheimer's Disease: An analysis controlling for tobacco industry affiliation. J Alzheimers Dis. 2010; 19:465–480. [PubMed: 20110594]
55. Brun A, Englund E. A white matter disorder in dementia of the Alzheimer type: A pathoanatomical study. Ann Neurol. 1986; 19:253–262. [PubMed: 3963770]
56. Englund E, Brun A, Ailing C. White matter changes in dementia of Alzheimer's type. Biochemical and neuropathological correlates. Brain. 1988; 111(Pt 6):1425–1439. [PubMed: 3208064]
57. de la Monte SM. Quantitation of cerebral atrophy in preclinical and end-stage Alzheimer's disease. Arm Neurol. 1989; 25:450–459.
58. Amlien IK, Fjell AM. Diffusion tensor imaging of white matter degeneration in Alzheimer's disease and mild cognitive impairment. Neuroscience. 2014; 276:206–215. [PubMed: 24583036]
59. Duncan GW, Firbank MJ, O'Brien JT, Burn DJ. Magnetic resonance imaging: A biomarker for cognitive impairment in Parkinson's disease? Mov Disord. 2013; 28:425–438. [PubMed: 23450518]
60. Roman G, Pascual B. Contribution of neuroimaging to the diagnosis of Alzheimer's disease and vascular dementia. Arch Med Res. 2012; 43:671–676. [PubMed: 23142262]
61. Jones RS, Waldman AD. 1H-MRS evaluation of metabolism in Alzheimer's disease and vascular dementia. Neurol Res. 2004; 26:488–495. [PubMed: 15265265]

62. de la Monte SM. Disproportionate atrophy of cerebral white matter in chronic alcoholics. Arch Neurol. 1988; 45:990–992. [PubMed: 3415529]
63. de la Monte SM, Kril JJ. Human alcohol-related neuropathology. Acta Neuropathol. 2014; 127:71–90. [PubMed: 24370929]
64. Harper C, Dixon G, Sheedy D, Garrick T. Neuropathological alterations in alcoholic brains. Studies arising from the New South Wales Tissue Resource Centre. Prog Neuropsychopharmacol Biol Psychiatry. 2003; 27:951–961. [PubMed: 14499312]
65. Kril JJ, Macdonald V, Patel S, Png F, Halliday GM. Distribution of brain atrophy in behavioral variant frontotemporal dementia. J Neurol Sci. 2005; 232:83–90. [PubMed: 15850587]
66. Rais M, Cahn W, Van Haren N, Schnack H, Caspers E, Hulshoff Pol H, Kahn R. Excessive brain volume loss over time in cannabis-using first-episode schizophrenia patients. Am J Psychiatry. 2008; 165:490–496. [PubMed: 18281413]
67. Witschi H, Espiritu I, Suffia M, Pinkerton KE. Expression of cyclin D1/2 in the lungs of strain A/J mice fed chemopreventive agents. Carcinogenesis. 2002; 23:289–294. [PubMed: 11872634]
68. Gordon T, Bosland M. Strain-dependent differences in susceptibility to lung cancer in inbred mice exposed to mainstream cigarette smoke. Cancer Lett. 2009; 275:213–220. [PubMed: 19118942]
69. March TH, Wilder JA, Esparza DC, Cossey PY, Blair LF, Herrera LK, McDonald JD, Campen MJ, Mauderly JL, Seagrave J. Modulators of cigarette smoke-induced pulmonary emphysema in A/J mice. Toxicol Sci. 2006; 92:545–559. [PubMed: 16699168]
70. Agarwal AR, Yin F, Cadenas E. Short-term cigarette smoke exposure leads to metabolic alterations in lung alveolar cells. Am J Respir Cell Mol Biol. 2014; 51:284–293. [PubMed: 24625219]
71. Agarwal AR, Zhao L, Sancheti H, Sundar IK, Rahman I, Cadenas E. Short-term cigarette smoke exposure induces reversible changes in energy metabolism and cellular redox status independent of inflammatory responses in mouse lungs. Am J Physiol Lung Cell Mol Physiol. 2012; 303:L889–L898. [PubMed: 23064950]
72. Groman E, Blauensteiner D, Kunze U, Schoberberger R. Carbon monoxide in the expired air of smokers who smoke so-called “light” brands of cigarettes. Tob Control. 2000; 9:352. [PubMed: 11203248]
73. Bergkvist A, Rusnakova V, Sindelka R, Garda JM, Sjogreen B, Lindh D, Forootan A, Kubista M. Gene expression profilling–Clusters of possibilities. Methods. 2010; 50:323–335. [PubMed: 20079843]
74. Team RC. R: A language and environment for statistical computing. R Foundation for Statistical Computing; 2015.
75. Prockop LD, Naidu KA. Brain CT and MRI findings after carbon monoxide toxicity. J Neuroimaging. 1999; 9:175–181. [PubMed: 10436761]
76. Federal Register, Online (4343). Review of national ambient air quality standards for carbon monoxide: Final Rule FR Doc N: 2011-21359. Environmental Protection Agency. 2011; 79(169): 5429. 3–5.
77. Stepanov I, Hecht SS. Tobacco-specific nitrosamines and their pyridine-N-glucuronides in the urine of smokers and smokeless tobacco users. Cancer Epidemiol Biomarkers Prev. 2005; 14:885–891. [PubMed: 15824160]
78. Stepanov I, Hecht SS. Detection and quantitation of N′-nitrosonornicotine in human toenails by liquid chromatography-electrospray ionization-tandem mass spectrometry. Cancer Epidemiol Biomarkers Prev. 2008; 17:945–948. [PubMed: 18398035]
79. Tricker AR, Ditrich C, Preussmann R. N-nitroso compounds in cigarette tobacco and their occurrence in mainstream tobacco smoke. Carcinogenesis. 1991; 12:257–261. [PubMed: 1995191]
80. de la Monte SM, Tong M, Lawton M, Longato L. Nitrosamine exposure exacerbates high fat diet-mediated type 2 diabetes mellitus, non-alcoholic steatohepatrtis, and neurodegeneration with cognitive impairment. Mol Neurodegener. 2009; 4:54. [PubMed: 20034403]
81. Englund E, Brun A. White matter changes in dementia of Alzheimer’s type: The difference in vulnerability between cell compartments. Histopathology. 1990; 16:433–439. [PubMed: 2361659]
82. Englund E, Brun A, Persson B. Correlations between histopathologic white matter changes and proton MR relaxation times in dementia. Alzheimer Dis Assoc Disord. 1987; 1:156–170. [PubMed: 3453747]

83. Bartzokis G, Sultzer D, Lu PH, Nuechterlein KH, Mintz J, Cummings JL. Heterogeneous age-related breakdown of white matter structural integrity: Implications for cortical “disconnection” in aging and Alzheimer’s disease. Neurobiol Aging. 2004; 25:843–851. [PubMed: 15212838]
84. Sjobeck M, Englund E. Glial levels determine severity of white matter disease in Alzheimer’s disease: A neuropathological study of glial changes. Neuropathol Appl Neurobiol. 2003; 29:159–169. [PubMed: 12662323]
85. Sjobeck M, Haglund M, Englund E. Decreasing myelin density reflected increasing white matter pathology in Alzheimer’s disease–a neuropathological study. Int J Geriatr Psychiatry. 2005; 20:919–926. [PubMed: 16163742]
86. Wang DS, Bennett DA, Mufson EJ, Mattila P, Cochran E, Dickson DW. Contribution of changes in ubiquitin and myelin basic protein to age-related cognitive decline. Neurosci Res. 2004; 48:93–100. [PubMed: 14687885]
87. Boulanger JJ, Messier C. From precursors to myelinating oligodendrocytes: Contribution of intrinsic and extrinsic factors to white matter plasticity in the adult brain. Neuroscience. 2014; 269C:343–366.
88. Campagnoni AT, Macklin WB. Cellular and molecular aspects of myelin protein gene expression. Mol Neurobiol. 1988; 2:41–89. [PubMed: 3077065]
89. Gordon MN, Kumar S, Espinosa de los Monteros A, Scully S, Zhang MS, Huber J, Cole RA, de Vellis J. Developmental regulation of myelin-associated genes in the normal and the myelin deficient mutant rat. Adv Exp Med Biol. 1990; 265:11–22. [PubMed: 1696059]
90. Le Bras B, Chatzopoulou E, Heydon K, Martinez S, Ikenaka K, Prestoz L, Spassky N, Zalc B, Thomas JL. Oligodendrocyte development in the embryonic brain: The contribution of the plp lineage. Int J Dev Biol. 2005; 49:209–220. [PubMed: 15906234]
91. Bordner KA, George ED, Carlyle BC, Duque A, Kitchen RR, Lam TT, Colangelo CM, Stone KL, Abbott TB, Mane SM, Nairn AC, Simen AA. Functional genomic and proteomic analysis reveals disruption of myelin-related genes and translation in a mouse model of early life neglect. Front Psychiatry. 2011; 2:18. [PubMed: 21629843]
92. Ghosh A, David S. Neurits growth-inhibitory activity in the adult rat cerebral cortical gray matter. J Neurobiol. 1997; 32:671–683. [PubMed: 9183745]
93. Nash M, Pribiag H, Fournier AE, Jacobson C. Central nervous system regeneration inhibitors and their intracellular substrates. Mol Neurobiol. 2009; 40:224–235. [PubMed: 19763907]
94. Skaper SD. Neuronal growth-promoting and inhibitory cues in neuroprotection and neuroregeneration. Ann N Y Acad Sci. 2005; 1053:376–385. [PubMed: 16179543]
95. Skaper SD. Neuronal growth-promoting and inhibitory cues in neuroprotection and neuroregeneration. Methods Mol Biol. 2012; 846:13–22. [PubMed: 22367797]
96. Webb AE, Brunet A. FOXO transcription factors: Key regulators of cellular quality control. Trends Biochem Sci. 2014; 39:159–169. [PubMed: 24630600]
97. Habener JF, Kemp DM, Thomas MK. Minireview: Transcriptional regulation in pancreatic development. Endocrinology. 2005; 146:1025–1034. [PubMed: 15604203]
98. Syed YA, Baer AS, Lubec G, Hoeger H, Widhalm G, Kotter MR. Inhibition of oligodendrocyte precursor cell differentiation by myelin-associated proteins. Neurosurg Focus. 2008; 24:E5.
99. Croizier S, Amiot C, Chen X, Presse F, Nahon JL, Wu JY, Fellmann D, Risold PY. Development of posterior hypothalamic neurons enlightens a switch in the prosencephalic basic plan. PLoS One. 2011; 6:e28574. [PubMed: 22194855]

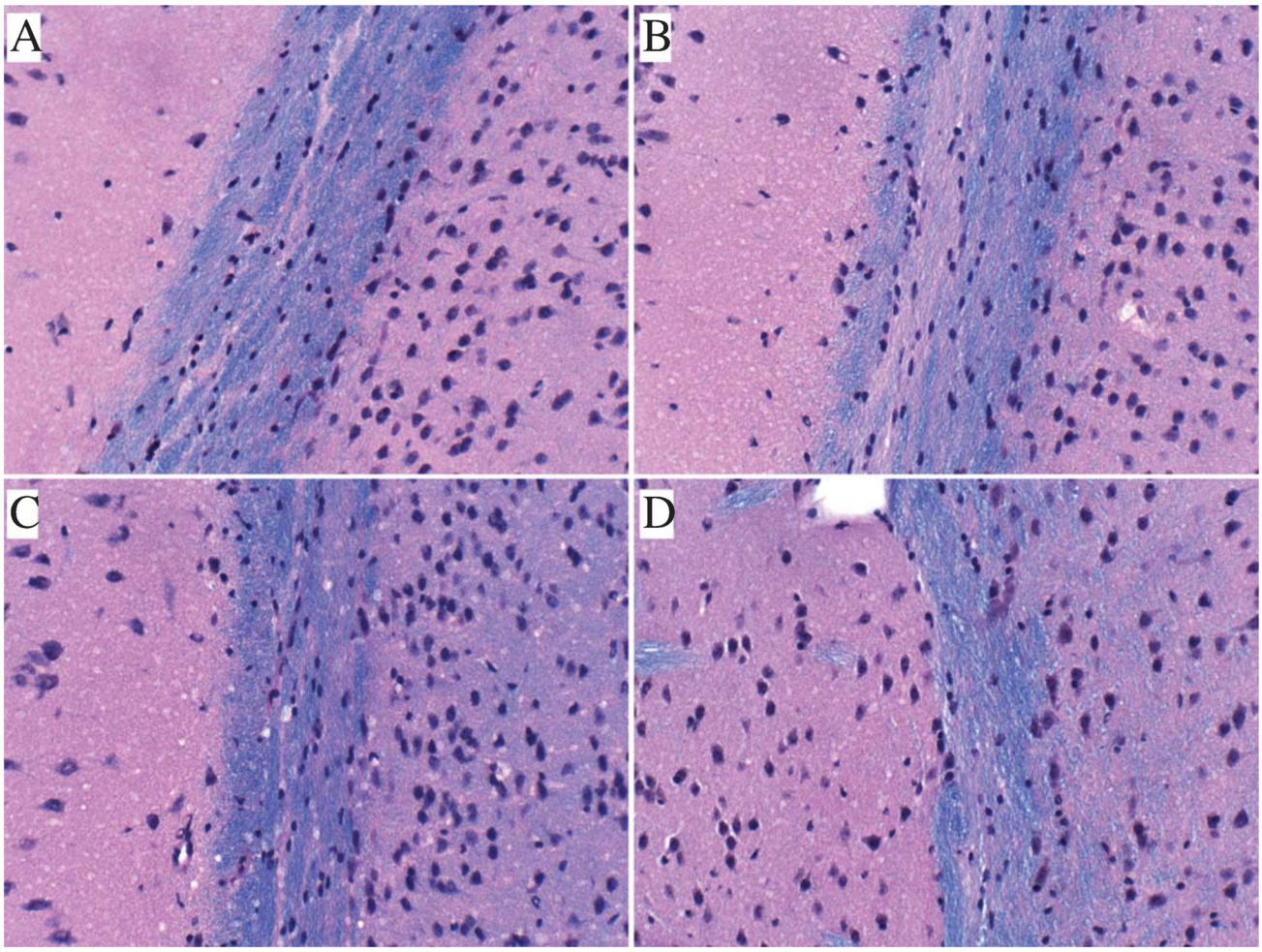

Fig. 1.

Effects of CS exposures on white matter histology. Formalin fixed, paraffin-embedded histological sections (8 μm thick) of frontal lobe corpus callosum from A8 control (A), CS4 (B), CS8 (C), or CS8 + R (D) mice were simultaneously stained with Luxol Fast Blue (LFB- for myelin). Hematoxylin and Eosin. CS4, CS8, and CS8 + R exposures were associated with thinning and pallor of myelin staining (blue) relative to control. Original magnifications = 100x; Scale bar = 50 μm.

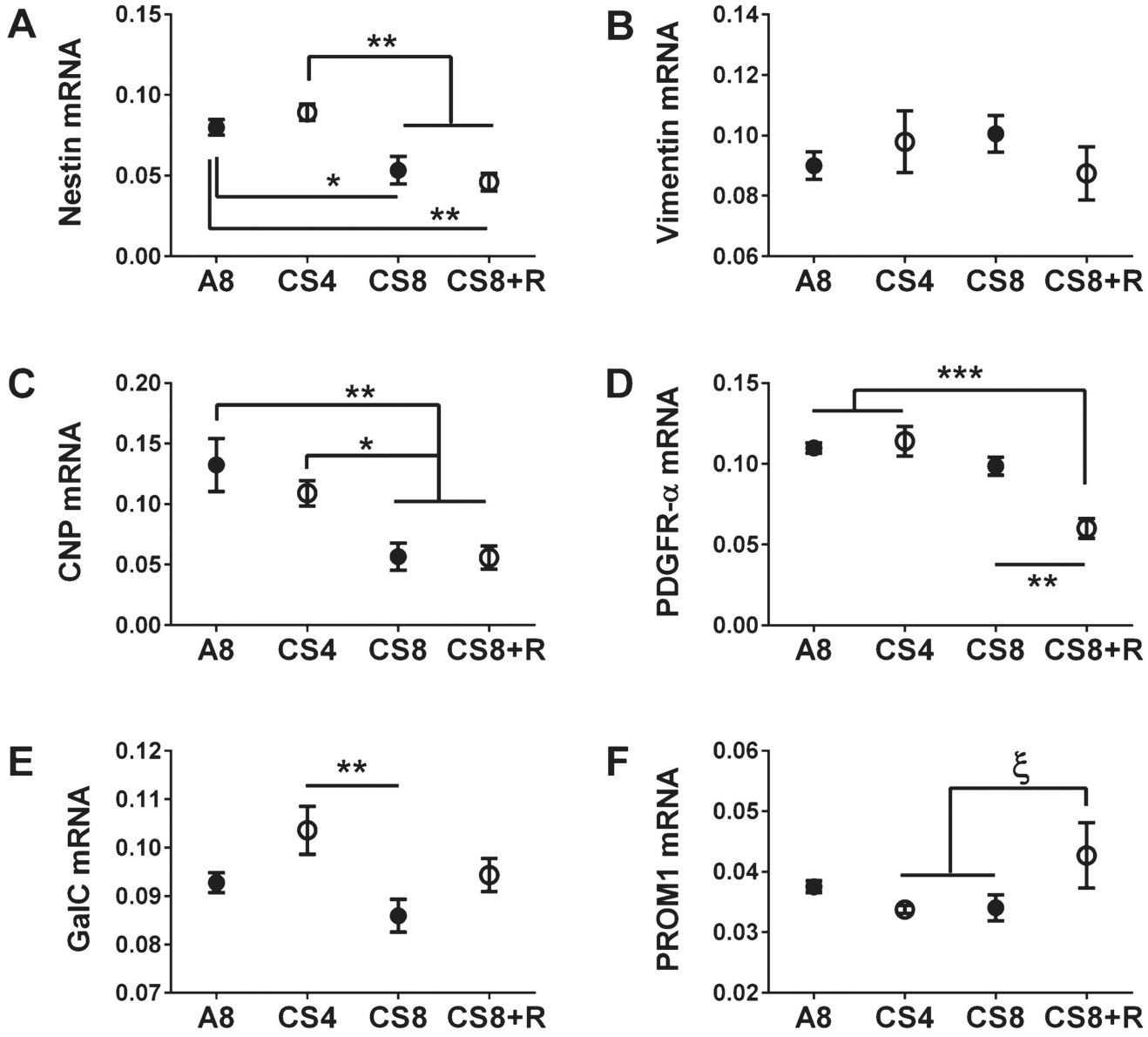

Fig. 2.

CS exposure effects on frontal lobe expression of immature oligodendroglial genes. mRNA levels of Nestin (A), Vimentin (B), CNP (2′,3′-cyclic nucleotide 3′ phosphodiesterase) (C), PDGFR-α (Platelet Derived Growth Factor Receptor, alpha polypeptide) (D), GalC (galactocerebrosidase) (E), and PROM 1 (Prominin 1) (F) were measured using targeted PCR arrays. Gene expression was calculated using the $^{\Delta\Delta}C_t$ method with results normalized to HPRT1. Inter-group comparisons were made by one-way ANOVA (Table 1) with the Tukey post-test (*$p < 0.05$; **$p < 0.01$; ***$p < 0.001$, $^{\xi}0.05 < p < 0.10$).

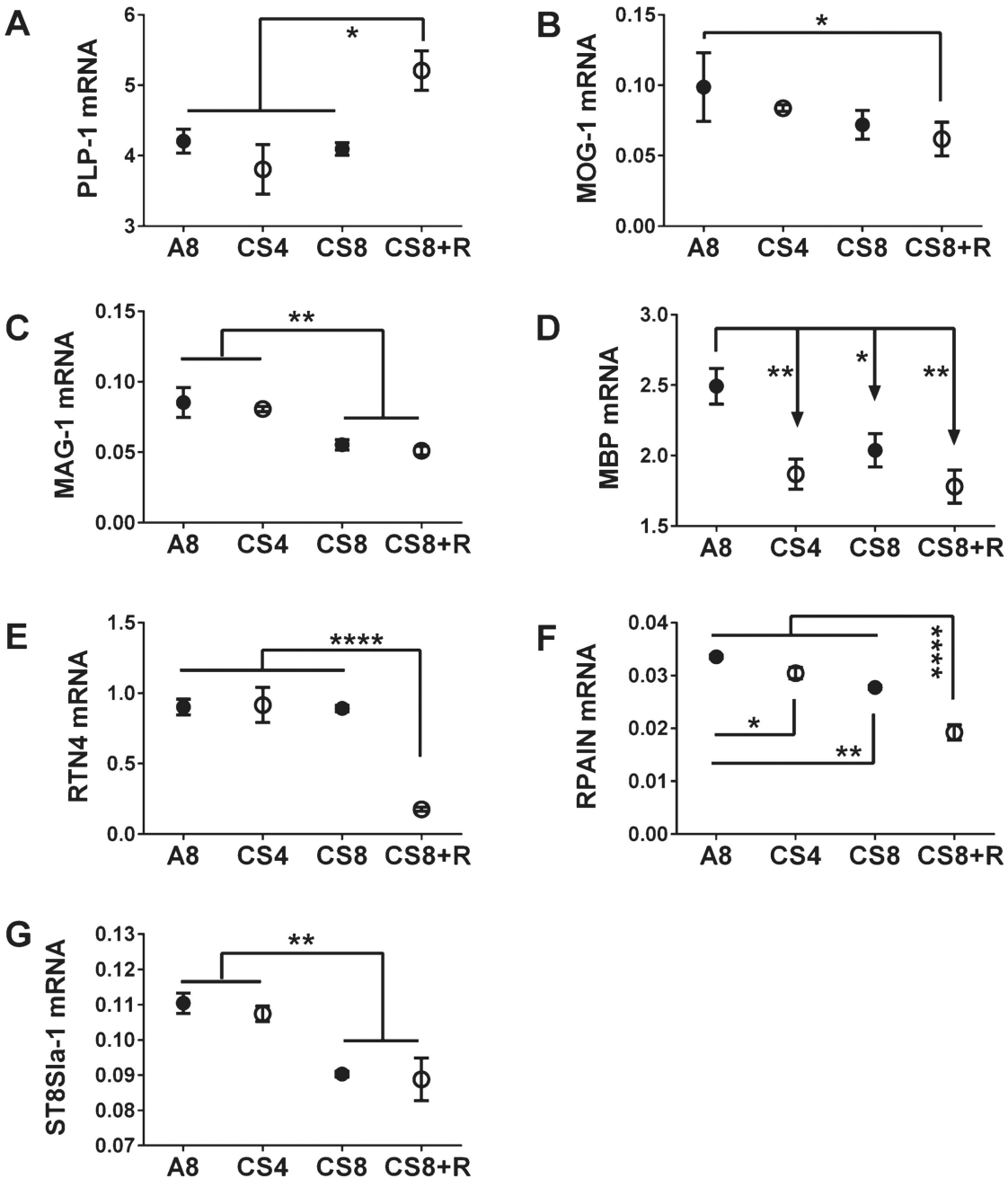

Fig. 3.

CS exposure effects on frontal lobe expression of mature oligodendroglial genes. mRNA levels of PLP-1 (proteolipid protein 1) (A), MOG-1 (myelin oligodendrocyte glycoprotein-1) (B), MAG-1 (myelin associated glycoprotein-1) (C), MBP (myelin basic protein) (D), RTN4 (reticulin 4) (E), RPAIN (RPA interacting protein) (F), and ST8S1a-1 (ST8 alpha-N-acetyl-neuraminide alpha-2,8-sialyllransferase 1) (G) were measured using targeted PCR arrays, and calculated using the $^{\Delta\Delta}C_t$ method with results normalized to HPRT1. Inter-group comparisons were made by one-way ANOVA (Table 1) with the Tukey post-test (*$p < 0.05$; **$p < 0.01$; ****$p < 0.0001$).

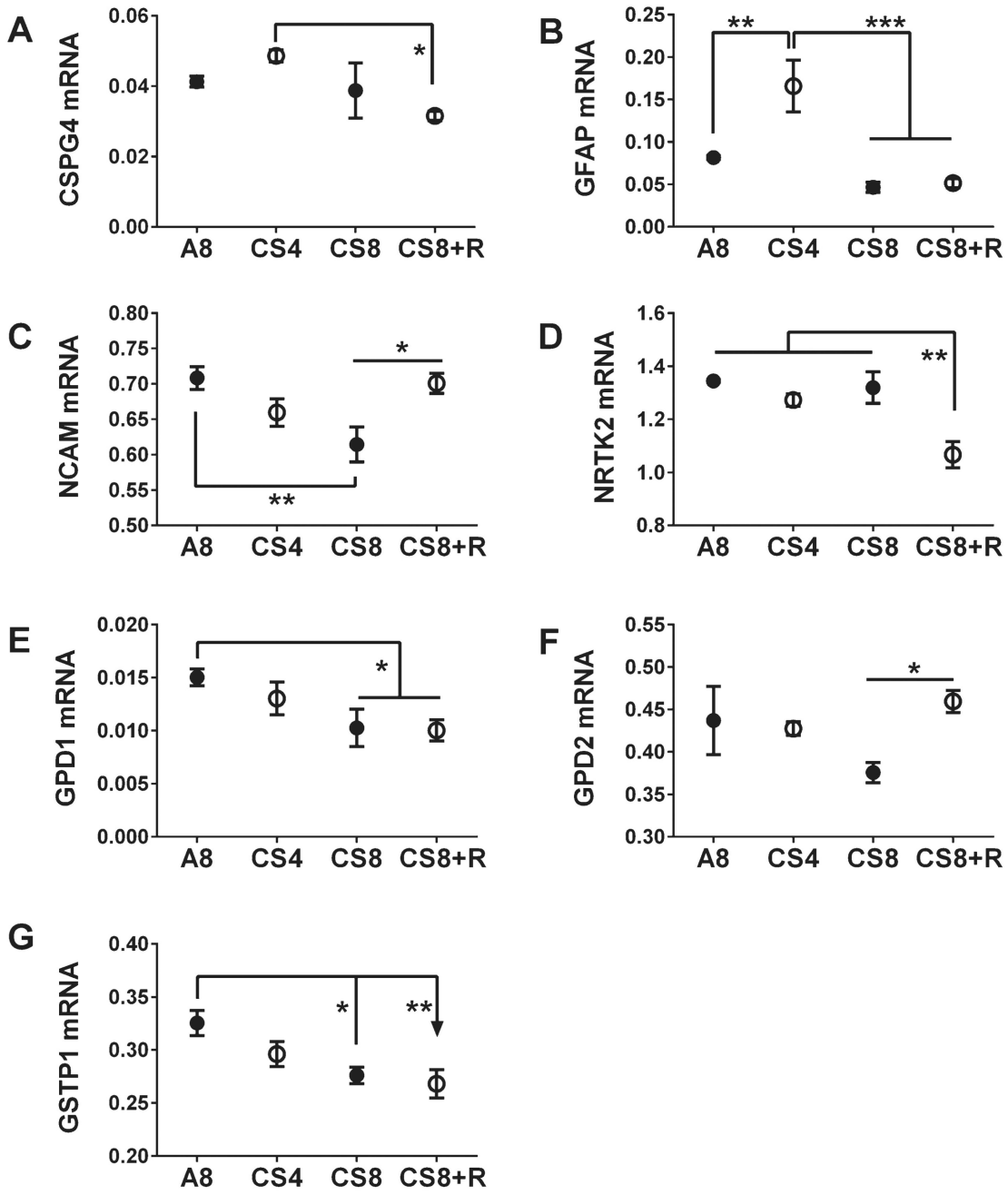

Fig. 4.

CS exposure effects on frontal lobe neuronal/glial gene expression in the temporal lobe. CSPG4 (Chondroitin sulfate proteoglycan 4) (A), GFAP (Glial fibrillary acidic protein) (B), NCAM (neural cell adhesion molecule 1) (C), NRTK2 (Neurotrophic receptor tyrosine kinase type 2) (D), GPD1 (Glycerol-3-phosphate dehydrogenase 1 (Soluble)) (E), GPD2 (Glycerol-3-phosphate dehydrogenase 2 (mitochondrial)) (F), and GSTP1 (Glutathione S-transferase pi 1) (G), mRNA levels were measured using custom targeted PCR arrays. Inter-group comparisons were made by one-way ANOVA (Table 1) with the Tukey post-test (*$p < 0.05$; **$p < 0.01$; ***$p < 0.001$).

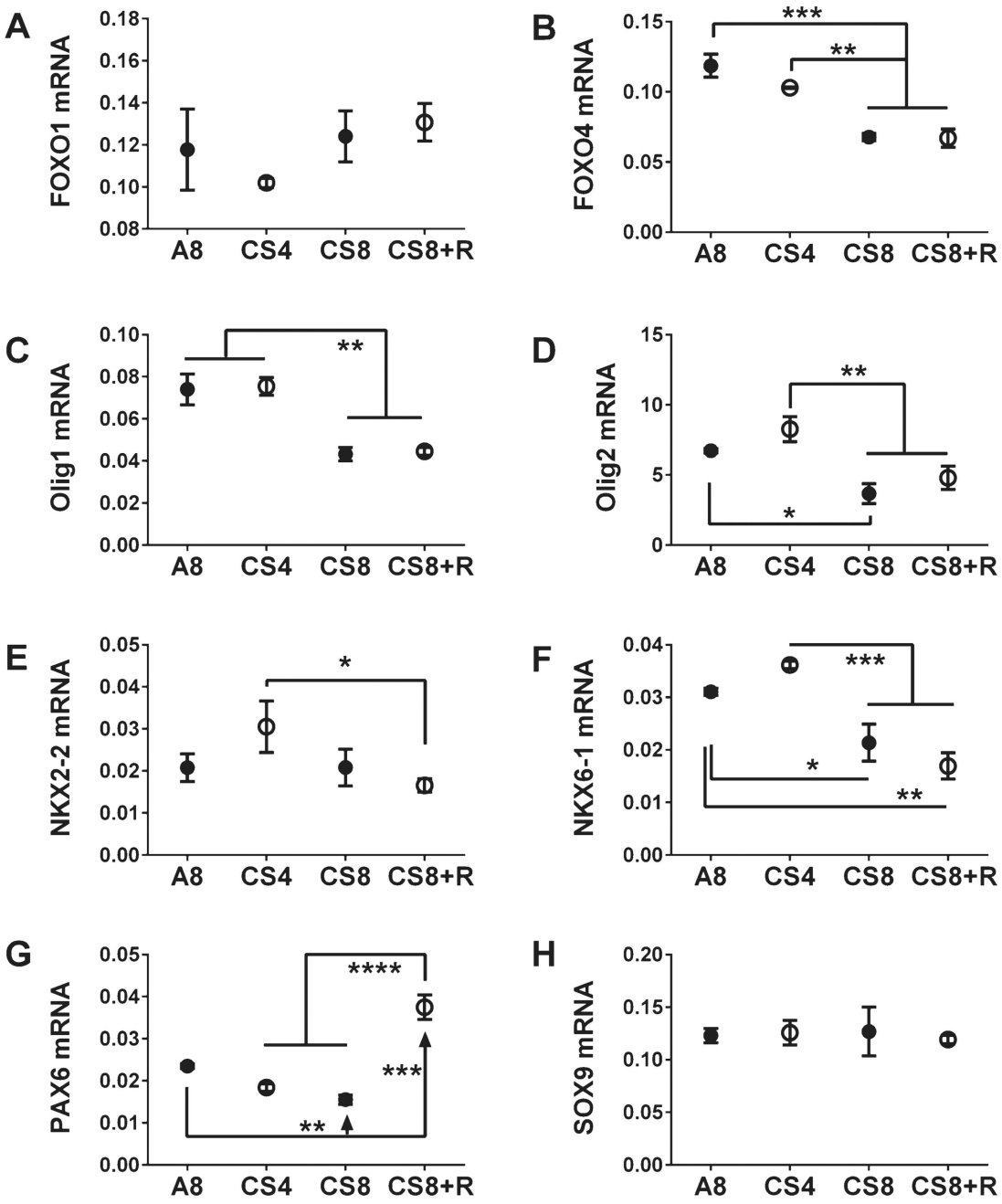

Fig. 5.

CS exposure effects on frontal lobe expression of transcription factor genes. The mRNA levels of FOXO1 (Forkhead Box O1) (A), FOXO4 (Forkhead Box O4) (B), Olig1 (Oligodendrocyte transcription factor 1) (C), Olig2 (Oligodendrocyte transcription factor 2) (D), NKX2-2 (NK2 Homeobox 2) (E), NKX6-1 (NK6 Homeobox 1) (F), PAX6 (Paired box 6) (G), and SOX9 (Sex determining region Y-Box 9) (H) were measured using targeted PCR arrays, and results were calculated using the $^{\Delta\Delta}C_t$ method after normalizing to HPRT1. Inter-group comparisons were made by one-way ANOVA (Table 1) with the Tukey post-test (*p < 0.05; **p < 0.01; ***p < 0.001; ****p < 0.0001).

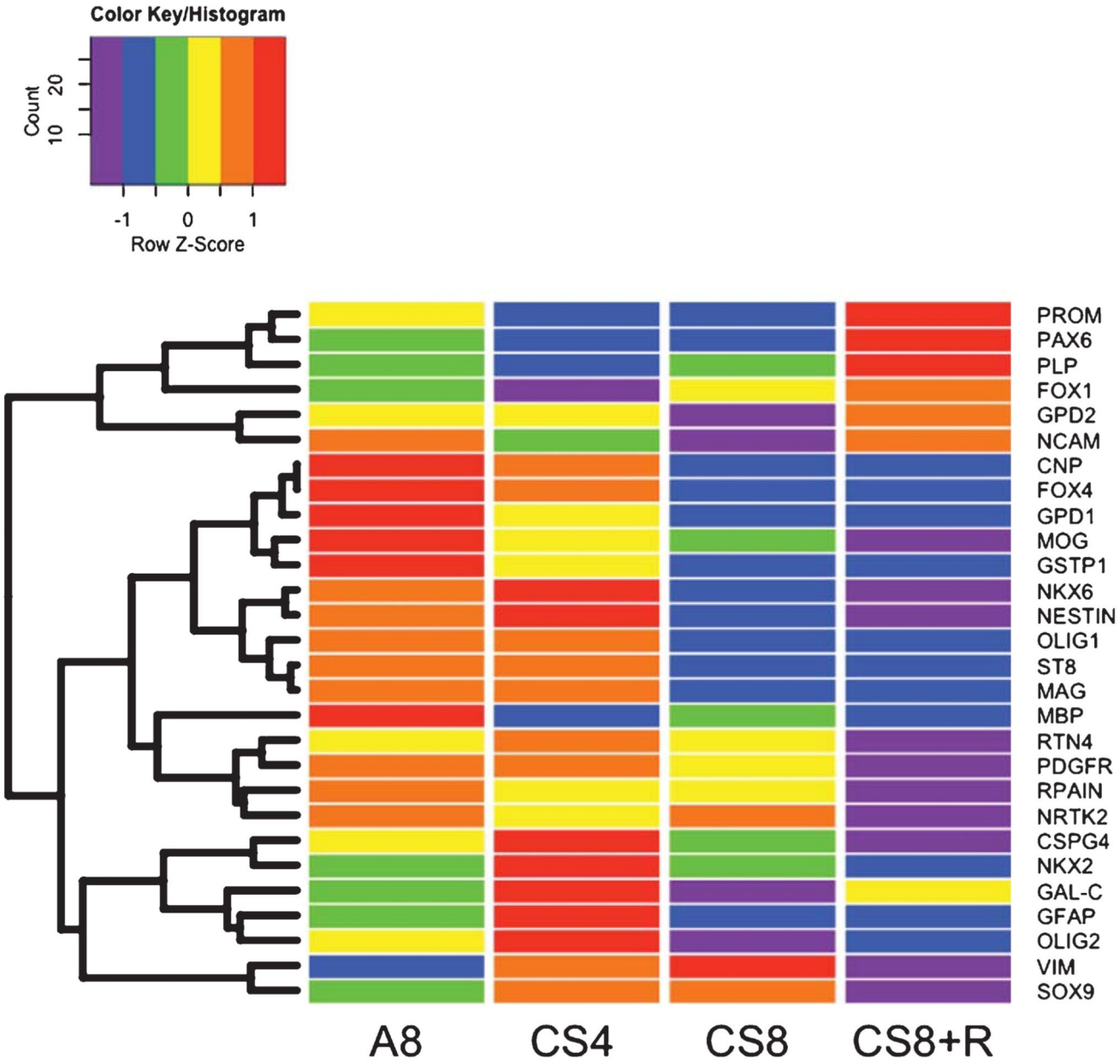

Fig. 6.

Heatmap illustrating hierarchical clustering of genes according to patterns of expression. The heatmap was generated using Version 3.2 of R software. Results shown with the 6-color palette correspond to z-scores, which were scaled to have a mean of 0 and S.D. of 1. A hierarchical clustering algorithm was applied using the Euclidean distance function on the overall table to display a dendrogram of mRNAs. A8 = control room air exposed × 8 weeks; CS4 = cigarette smoke exposed × 4 weeks; CS8 = cigarette smoke exposed × 8 weeks; CS8 + R = cigarette smoke exposed × 8 weeks followed by 2 weeks recovery in room air.

Table 1

Smoking and smoking withdrawal effects on frontal lobe expression of glial and neuronal genes

mRNA	F-ratio	*p*-value
Immature Oligodendroglia		
CNP	7.35	0.01
GAL-C	4.05	0.05
Nestin	11.32	0.003
PDGFR-α	14.94	0.0012
PROM	1.97	N.S.
Vimentin	0.065	N.S.
Mature Oligodendroglia		
MAG-1	8.68	0.0068
MBP	7.290	0.011
MOG	*3.56*	*0.067*
PLP	6.21	0.017
RPAIN	44.25	< 0.0001
RTN4	27.37	0.0001
ST8	10.06	0.004
Neuroglial Markers		
CSPG4	*2.90*	*0.10*
GFAP	12.13	0.002
GPD1	*3.19*	*0.084*
GPD2	2.51	N.S.
GSTP1	5.05	0.029
NCAM	5.19	0.028
NTRK2	9.65	0.005
Transcription Factors		
FOXO1	1.05	N.S.
FOXO4	22.87	0.0003
NKX2-2	2.01	N.S.
NKX6	15.73	0.001
Olig1	14.80	0.001
Olig2	8.33	0.007
PAX6	34.69	< 0.0001
SOX9	0.06	N.S.

Frontal lobe RNA was analyzed using a targeted PCR array to examine CS effects on oligodendroglial/white matter myelin-associated gene expression. Data were analyzed by one-way ANOVA; the corresponding F-ratios and *P*-values are tabulated. The *post hoc* Tukey test was used to further identify statistically significant specific inter-group differences. Those results are shown within individual panels of Figs. 2–5. See Supplementary Table 1 for abbreviations and gene functions.